Journal for ImmunoTherapy of Cancer

Germline whole-exome sequencing reveals *FOXP3*-related gene variants conferring urinary cancer susceptibility and associated with immune escape

Bing-Jian Feng ,[1] Wendy Kohlmann,[2,3] David A Nix,[2] Aaron Atkinson,[2] Kenneth M Boucher,[2] Courtney Carroll ,[1] Chris J Stubben,[2] Jill Kolesar,[4] Eric A Singer,[5,6] Gregory Riedlinger,[5] Stephen Edge,[7] Kamal Kant Sahu,[2,8] Michelle Churchman,[9] Laura Graham,[10] Bodour Salhia,[11,12] Alejandro Sanchez,[2] Yousef Zakharia ,[13] Bryan P Schneider,[14] Rohit Jain,[15] Lindsey Byrne ,[6] Christopher A Moskaluk,[16] Kenneth Nepple,[13,17] Ahmad Shabsigh,[6] Jad Chahoud,[18] Bradley R Cairns,[2] Sumati Gupta [2,19]

To cite: Feng B-J, Kohlmann W, Nix DA, *et al*. Germline whole-exome sequencing reveals *FOXP3*-related gene variants conferring urinary cancer susceptibility and associated with immune escape. *Journal for ImmunoTherapy of Cancer* 2025;**13**:e010417. doi:10.1136/jitc-2024-010417

► Additional supplemental material is published online only. To view, please visit the journal online (https://doi.org/10.1136/jitc-2024-010417).

Accepted 24 August 2025

Check for updates

For numbered affiliations see end of article.

Correspondence to
Dr Sumati Gupta;
Sumati.Gupta@hci.utah.edu

ABSTRACT

Background The heritability of urinary tract cancer (UTC) remains unexplained by known pathogenic germline variants, and the influence of germline variants on treatment response to immune checkpoint inhibition (ICI) has yet to be fully elucidated.

Methods In this case–control study, we performed a germline whole-exome sequencing of 810 UTC patients from the Oncology Research Information Exchange Network. A rare-variant burden test was conducted on the 810 patients and 2354 healthy controls from the Centre d'Etudes du Polymorphisme Humain families, the University of Utah Heritage 1000 Projects, and the 1000 Genomes Project, stratified into discovery and confirmation sets. We used a gene set-based rare-variant association test (GSRVAT) with near-match confirmation, testing for the association of pathways with UTC susceptibility and accounting for multiple testing. We then studied the impact of the identified pathways on tumor biology and clinical course among the 810 cases by analyzing their tumor exomes, transcriptomes, and clinical features.

Results GSRVAT revealed forkhead box p3 (*FOXP3*) as a susceptibility pathway in 16% of patients with UTC, with an epistasis with DNA mismatch repair. Carriers of germline truncating variants in *FOXP3*-related susceptibility genes exhibited decreased tumor *FOXP3* expression levels, which were associated with a cold tumor microenvironment and significantly reduced overall and progression-free survival following ICI.

Conclusions Germline variants in a set of *FOXP3*-related genes confer inherent susceptibility to UTC and contribute to resistance against ICI. The immune-evading trait resulting from these variants and the downregulation of *FOXP3* expression introduce a novel avenue for personalized medicine through germline and tumor sequencing.

WHAT IS ALREADY KNOWN ON THIS TOPIC

⇒ The influence of germline variants on treatment response to immune checkpoint inhibition in urinary tract cancers has yet to be elucidated.

WHAT THIS STUDY ADDS

⇒ This study identified that forkhead box p3 (*FOXP3*)-related genes confer inherent cancer susceptibility and immune-evasive qualities to the tumors. Germline variants lead to reduced *FOXP3* expression levels in tumors, which in turn are associated with a worse prognosis after immunotherapy.

HOW THIS STUDY MIGHT AFFECT RESEARCH, PRACTICE OR POLICY

⇒ Germline sequencing of the *FOXP3*-related genes and expression profiling of *FOXP3* in tumors can guide immunotherapy decisions.

INTRODUCTION

Bladder cancer (BC) is the most common urinary tract cancer (UTC), frequently recurring and progressing with a high mortality risk in those over 70 years old.[1] While effective combination therapies for advanced UTC exist, their toxicity limits use in older adults.[2 3] Immune checkpoint inhibition (ICI) alone is more tolerable but less effective.[4–7] Targeting tumor driver mutations in UTC has limited efficacy or short-lived benefit,[8–10] suggesting additional oncogenic drivers.

Aging and carcinogen exposure are key risk factors for UTC,[11] but there is also a pattern of familial clustering[12 13] and an estimated 30% genetic heritability[14] that cannot be fully explained by shared environmental risks or known disease genes.[15 16] Genome-wide association studies and whole-exome sequencing (WES) suggest that host factors contribute to BC tumor biology.[17–21] Therefore, findings from susceptibility studies have the potential to reveal pathways that predict treatment response and disease outcomes.

To bridge the gap between known heritability and genetic risks and better understand the drivers of tumor biology, we leveraged the comprehensive Oncology Research Information Exchange Network (ORIEN) dataset, encompassing clinically annotated germline WES, tumor WES, and tumor RNA sequencing (RNA-seq) data for patients from multiple cancer centers in the USA. This is the first report of a genetic association study to identify rare germline variants in *FOXP3*-related genes as associated with UTC susceptibility and their impact on tumor biology and disease progression following ICI.

PATIENTS AND METHODS

Reporting

The STrengthening the REporting of Genetic Association Studies reporting guidelines were used for this manuscript.[22]

Study population

The ORIEN consortium represents a nationwide network of 19 cancer centers. The ORIEN Avatar program conducts germline WES, tumor WES, and tumor RNA-seq to research and match patients to clinical trials as previously described.[23 24] Details regarding data sources for the variables used in this study are listed on the ORIEN website at https://www.oriencancer.org.[25] Our study included 810 patients with primary sites of cancer in the urinary tract (bladder, renal pelvis, ureter, urethra) and excluded any kidney cancer cases unless they were urothelial by histology. As illustrated in figure 1, we stratified the 810 germline WES data into discovery and confirmation sets.

Sequencing

The sequencing experiments and primary analysis of the sequencing data of the ORIEN Avatar program are described in Kohlmann *et al*.[26]

In the discovery set, 354 UTC cases were compared with 371 healthy, unrelated controls from the Centre d'Etudes du Polymorphisme Humain families and the University of Utah Heritage 1000 (H1K) Projects. The sequencing of H1K samples was described in Ostrander *et al*.[27] In brief, DNA was extracted from blood or saliva. Genomes were prepared using TruSeq DNA PCR-free libraries (Illumina) and run on the Illumina HiSeq X Ten System at a minimum of ×60 median whole-genome coverage. The same bioinformatics pipeline was used to analyze cases and control data, starting from BAM files. Paired-end reads were aligned to the GRCh38 reference genome using Burrows-Wheeler Aligner V.0.7.10. Variants in both cases and controls were jointly called using the Sentieon software.

In the confirmation set, germline variants in 456 cases were jointly called with 1983 WES data from the 1000 Genomes Project using the Sentieon software.

Tumor exome sequencing data from the ORIEN Avatar program were processed by the TNRunner workflow of the USeq software (https://github.com/HuntsmanCancerInstitute). This workflow aligned tumor and germline DNA sequencing reads to GRCh38 and called variants by Illumina's Strelka2 Small Variant Caller. Somatic mutations were extracted by subtracting germline variants from tumor variants. Genome-wide tumor mutation burden (TMB) was calculated from non-synonymous variants. To ensure comparability of the TMB among patients, we performed a joint variant calling by the GATK package and then excluded variants if the missing rate was >10% or the variant was outside the callable regions for 95% of the samples.

The TNRunner RnaAlignQC workflow was run on each tumor RNA-seq dataset. This workflow uses CutAdapt V.3.4 to remove adapter sequences, STAR V.2.7.9a[28] to align reads to the human GRCh38 Ensembl 106 reference, and featureCounts subread 2.0.3[29] to assign reads to annotated genes.

In patients who had multiple tumor specimens, we selected one specimen per patient to analyze tumor WES and tumor RNA-seq (online supplemental note 1).

Quality control (QC) of data

In the discovery set (n=354), the germline analyses excluded 18 cases with a high genotype missing rate (figure 1). The remaining 336 cases were compared with 364 healthy individuals (figure 1). Cryptic relatedness, or unexpected genetic correlation between two or more cases, was inferred using the program KING (Kinship-based INference for Genome-wide association studies). In cases where multiple individuals were genetically related, only one individual, the one with the lowest genotype missing rate, was included in the analysis. In the confirmation set (n=456), one case was excluded due to cryptic relatedness, and an additional 62 cases were eliminated because of a high missing rate (figure 1). Gene-based and gene set-based rare-variant association tests (GSRVATs) on the discovery set yielded p values with the expected distribution and no evidence of type 1 error inflation, affirming the high quality of the data (online supplemental figure S1).

Among the 780 samples that underwent tumor WES, 730 (93.6%) were derived from specimens originating from primary sites, while the remainder were obtained from metastatic sites. The consistency of TMB across inferred ancestry categories was observed from a non-significant Kruskal-Wallis test (online supplemental figure S2).

The ORIEN data contained 554 tumor samples with RNA-seq data available. We excluded 52 samples due to missing clinical data and 11 duplicates. To mitigate technical variations and batch effects, we removed 43 non-primary tumor samples, 128 samples prepared by tagmentation, 1 sample exhibiting over 300 extreme

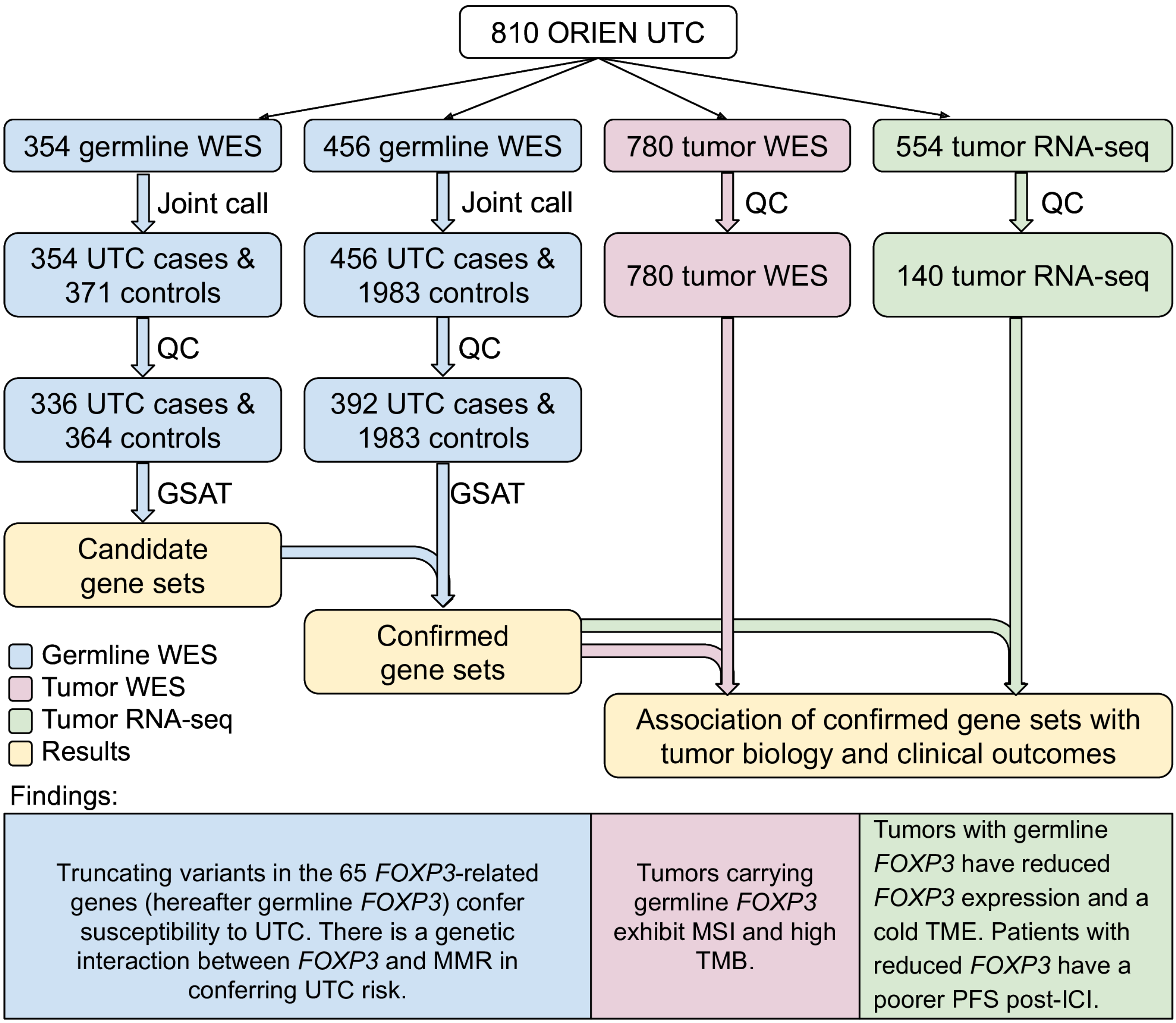

Figure 1 Study design. *FOXP3*, forkhead box p3; ICI, immune checkpoint inhibition; MSI, microsatellite instability; GSRVAT, gene set-based rare-variant association test;ORIEN, the Oncology Research Information Exchange Network; PFS, progression-free survival; QC, quality control; RNA-seq, RNA sequencing; TMB, tumor mutation burden; TME, tumor microenvironment; UTC, urinary tract cancer; WES, whole-exome sequencing.

count outliers, and 179 samples derived from formalin-fixed paraffin-embedded tissue specimens. This process resulted in the retention of 140 samples for subsequent analysis.

Medical Subject Headings (MeSH) terms over-represented in a gene set

To delineate the biological functions of a set of genes, we conducted a gene set over-representation analysis (GSOA) using the BioLitMine database[30] to identify MeSH terms that were over-represented among these genes. BioLitMine mesh2gene database (V.2023.2) was kindly provided by Dr Claire Yanhui Hu. From BioLitMine, we constructed a gene set database linking multiple *Homo sapiens* genes to each MeSH term in the Phenomena and Processes category. A total of 1157 MeSH terms were considered for GSOA after excluding 61 uninformative terms, 148 with fewer than 2 genes analyzed by WES, 112 with more than 2000 genes analyzed by WES, and 11 duplicates. Subsequently, we conducted a one-sided mid-p Fisher's exact test for each MeSH term based on a 2×2 contingency table and then corrected the p value by the Šidák procedure (Pc) to control the family-wise error rate. MeSH terms with Pc<0.05 were deemed significant.

Analysis of germline exomes

Variant annotation, filtering, and statistical analyses of WES data were conducted using the Variant Interpretation for Clinical Test or Research (VICTOR, http://

BJFengLab.org/) software suite[31] V.1.2 beta, built on 10 August 2023, and R V.4.3.1.

VICTOR performs a sandwich QC approach consisting of three stages: variant-wise QC, sample-wise QC, and variant-wise QC. This strategy ensures that the sample-wise QC is based on high-quality variants and that the variant-wise QC is based on high-quality samples. Variants were filtered out based on Variant Quality Score Recalibration, the FILTER column of the Variant Call Format (VCF) file, the missing rate (>10%), and an exact Hardy-Weinberg Equilibrium test within each ancestry group ($p<0.000001$). In both the rare-variant association test (RVAT) and the epistasis test involving the comparison of rare-variant burdens, samples with missing genotypes were excluded. This approach ensured comparability between cases and controls, effectively controlling type 1 errors.

Subsequently, VICTOR annotated and filtered variants and performed RVAT by Firth's penalized logistic regression. To account for population stratification, the VICTOR pipeline first inferred ancestry and then conducted association analyses separately within each ancestry group (African/African American, Admixed American, East Asian, Non-Finnish European, and South Asian). Within each ancestry, population substructure was adjusted using principal components calculated from a within-ancestry principal component analysis, with the number of components determined using the elbow method. Results from different ancestry groups were combined using Stouffer's method, with each group weighted by its effective sample size calculated as $4\times S\times T/(S+T)$, where S is the number of cases, and T is the number of controls.

Since variants were excluded if they had a low BayesDel deleteriousness score,[32] a high maximum allele frequency across populations, or a ClinVar classification as Benign or Likely Benign, a protective effect conferred by the remaining variants was not expected. Therefore, RVAT was one-sided. The genome-wide significance threshold was set at $p<0.05$ after Šidák correction for the number of genes or gene sets in the analysis. To select gene sets for confirmation, we calculated each gene set's false discovery rate (q value) and progressively reduced the q value threshold from 1 to 0 until fewer than ten gene sets remained. If more than 10 sets remained, only the first 10 sets were selected.

To assess epistasis between two pathways, we coded genotypes of the two pathways into a four-level variable, corresponding to (1) not carrying any variants, (2) carrying a germline variant in the first pathway, (3) carrying a germline variant in the second pathway, and (4) carrying germline variants in both pathways, respectively. Logistic regression was performed on this variable, using level 1 as the reference, adjusting for ancestry. We employed a stratified permutation to assess the statistical significance of epistasis. In this method, the germline carrier status of a pathway was independently shuffled within each stratum of individuals defined by affection status and ancestry, preserving the individual effects of each pathway while disrupting the correlation between them. An epistasis p value was then calculated as the proportion of instances where the shuffled data produced a higher odds ratio (OR) for the level 4 genotype than the unshuffled data. We randomly selected two gene sets from the human genome and computed the epistasis p value to validate this approach. This procedure was repeated 1000 times. The quantile–quantile plot of these p values confirmed the stratified permutation test's correct type 1 error rate (online supplemental figure S3).

Analysis of tumor transcriptomes

A total of 17 403 expressed genes were normalized using DESeq2, and *FOXP3* high-expression and low-expression groups, separated by the median value, were compared by linear regression, with gene expression as the outcome variable and *FOXP3* group as the predictor, adjusting for age and sex. Gene set enrichment analysis (GSEA) was performed on each gene's regression coefficient. We performed one-sided GSEA for positive and negative enrichment separately. The direction with a higher absolute enrichment score was chosen. This approach is more powerful than the two-sided GSEA when the association test results are skewed. A GSOA was also performed to validate this approach. This involved testing the over-representation of a gene set among nominally associated genes using Fisher's exact test separately for each direction of association. Gene sets for GSEA and GSOA were obtained from the MSigDB hallmark database and the TIMEx (Tumor-Immune Microenvironment deconvolution) program (http://timex.moffitt.org). The significance threshold was 0.05 after Šidák correction for the number of gene sets analyzed.

Overall survival (OS) was assessed using a Cox proportional hazards regression model, measuring the time from the initial UTC diagnosis to death or the last contact. Progression-free survival (PFS) by treatment type was calculated from the start of treatment to the first noted progression, including tumor growth on imaging, medication changes due to progression, metastasis, recurrence or the last contact, whichever occurred first. Loss to follow-up was treated as censoring.

Analysis of the Cancer Genome Atlas Urothelial Bladder Carcinoma (TCGA-BLCA) data

This dataset comprised tumor RNA-seq data on 408 urothelial bladder carcinoma samples.

RESULTS

Samples

The number of samples is described in figure 1. The UTC cases were predominantly European individuals (online supplemental tables S1 and S4). The mean follow-up times for OS, PFS following ICI, and PFS following platinum-based treatment were 38.0, 21.7, and 33.7 months, respectively. Among the 810 ORIEN samples, 804 had clinical data. The missing rate for each variable of interest is indicated in online supplemental figure S5 (804 minus the total number of patients at risk at time zero). Clinical features associated with OS, revealed through a single-variable Cox proportional hazards regression, included older age, higher stage, and neuroendocrine histological type (online supplemental figure S5). In the subsequent analyses, we included non-urothelial histology to ensure a comprehensive UTC study and a cohort that represents a real-world patient population.

Gene prioritization demonstrated DNA mismatch repair (MMR) genes

Gene-based RVAT on the discovery or confirmation set did not yield a genome-wide significance. A meta-analysis of both sets also failed to achieve genome-wide significance (online supplemental table S2). However, GSEA[33] on the meta-p values for deleterious variants revealed a noteworthy enrichment of American College of Medical Genetics and Genomics-recommended[34] cancer-related genes (p=0.024) (online supplemental table S3 and figure S6A). Further categorization of these cancer genes by mechanism showed significant enrichment of MMR genes (p=0.015) (online supplemental table S3 and figure S6B). In contrast, no significant enrichments were observed for homologous recombination repair (p=0.43), non-recombinational repair (p=0.70), base excision repair (p=0.30), or nucleotide excision repair genes (p=0.59).

GSRVAT identified *FOXP3*-related gene sets

Given the absence of a major gene contributing to UTC susceptibility, as evidenced by the gene-based RVAT, we conducted a GSRVAT, aggregating functionally related genes into a testing unit to enhance statistical power by accumulating each gene's individual effect. Intriguingly, the top 10 gene sets, ranked among the 11 786 analyzed sets in the analysis of truncating variants, exhibited functional correlations among themselves (table 1). Specifically, the second and fifth gene sets are linked to *FOXP3*, considering that scurfy mice are characterized by a non-functional *FOXP3*. To assess the biological correlation between these two gene sets quantitatively, we conducted a literature mining of 1157 unselected MeSH terms and calculated the enrichment of each term in each gene set, measured as log ORs. The correlation analysis of these log ORs between the two gene sets resulted in a Pearson's correlation coefficient of 0.91, with a 95% CI ranging from 0.90 to 0.92, confirming their biological correlation.

Notably, the association between these two sets cannot be attributed to the same genes, as there were no significantly overlapping genes between them (online supplemental table S4). This observation, that two *FOXP3*-related gene sets independently contributed to UTC predisposition, not only provides additional support for the involvement of *FOXP3* in UTC susceptibility but also suggests a high level of locus heterogeneity.

Given the locus heterogeneity in UTC susceptibility, we adopted a near-match approach at the confirmation stage. In this approach, instead of directly testing each candidate gene set on confirmatory samples, we expanded each candidate set to include a group of biologically correlated gene sets, identified through key phrase matching of gene set names. We then tested all gene sets within each group and selected the lowest p value, adjusting for multiple testing using the Šidák method. The adjusted p value was designated as the near-match confirmation p value (Pnmc) for the original candidate gene set. Using this approach, both the second and fifth gene sets achieved significant confirmation with Pnmc<0.005 (table 1).

The four *FOXP3*-related gene sets (including two candidate gene sets and two top gene sets from the near-match confirmation) comprised 65 unique genes with a p value<0.25 (online supplemental table S4 and S5). The limited overlap among these gene sets further corroborates the significant locus heterogeneity observed in UTC susceptibility. Among the 810 UTC patients, 127 (16%) had at least one truncating germline variant within the 65 *FOXP3*-related genes (figure 2A).

Epistasis between *FOXP3* and MMR gene sets

Carrying a germline variant in the 65-gene *FOXP3*-related gene set did not associate with UTC primary site, histology, stage, age at diagnosis, OS, or PFS. However, individuals harboring a truncating variant in one of the 65 genes exhibited an elevated TMB and increased microsatellite instability (MSI) (figure 2B,C).

The correlation between germline status of *FOXP3*-related genes and TMB and MSI led us to hypothesize a potential synergistic effect, or epistasis, between *FOXP3* and DNA repair pathways, particularly MMR genes, given the earlier gene prioritization findings. To evaluate this interaction, we conducted logistic regression using the 810 ORIEN UTC cases and 1000 Genomes Project controls. MMR genes (n=34) were sourced from the MSigDB database, disregarding their individual association with UTC, and excluding *PMS2* due to the potential presence of pseudogene mutations.

Relative to patients without variants in either pathway, having a deleterious variant in the MMR pathway alone did not exhibit a significant association with UTC (p=0.42). Conversely, harboring a truncating variant in the *FOXP3*-related genes alone resulted in an OR of 3.68, while carrying both MMR-related and *FOXP3*-related variants boosted the OR to 25.2 (table 2). A stratified permutation test (online supplemental note 1) assessed the *FOXP3*–MMR interaction as significant (p=0.043).

It is imperative to highlight that the observed synergy between *FOXP3* and MMR gene sets cannot be attributed to linkage disequilibrium, considering the dispersion of multiple genes across the genome (online supplemental figure S7) and the absence of co-occurrence of germline variants in *FOXP3*-related genes and MMR genes in healthy controls (p=0.99 by Fisher's exact test).

FOXP3 is associated with the tumor microenvironment (TME)

Literature mining of 1157 unselected MeSH terms showed that "TME" was the top-ranking and significantly

Table 1 Near-match confirmation of the top 10 gene sets identified from germline exomes

Discovery set			Confirmation set			
Candidate set*	**OR (95% CI)**	**P value†**	**Matches**	**Top matched set**	**OR (95% CI)**	**Pnmc‡**
FOXJ2 01	5.25 (2.29 to 12.0)	0.00004	2	FOXJ2 01	1.21 (0.13 to 11.1)	0.8132
Gavin ***FOXP3*** **targets cluster** P4	3.79 (1.77 to 8.11)	0.00031	7	Gavin *FOXP3* targets cluster P6	3.26 (1.66 to 6.38)	0.0020 **
Postsynaptic density	5.50 (2.01 to 15.1)	0.00046	4	Postsynaptic density membrane	4.86 (1.35 to 17.5)	0.031
GO **regulation of endocrine process**	9.60 (2.42 to 38.1)	0.00065	1	GO regulation of endocrine process	2.20 (0.72 to 6.70)	0.083
GSE23398 WT versus IL2 KO CD4 T-cell **scurfy mouse** DN	3.07 (1.55 to 6.09)	0.00065	2	GSE23398 WT versus IL2 KO CD4 T-cell scurfy mouse UP	2.03 (1.25 to 3.31)	0.0043 **
GSE37301 **CD4 T-cell versus granulocyte monocyte progenitor** UP	2.83 (1.50 to 5.37)	0.00070	2	GSE37301 CD4 T-cell versus granulocyte monocyte progenitor DN	1.14 (0.84 to 1.55)	0.35
GSE12366 **naive versus memory B-cell** UP	1.69 (1.22 to 2.33)	0.00074	10	GSE42724 naive versus memory B-cell DN	1.93 (1.25 to 2.98)	0.014
GSE22432 **CDC versus common DC progenitor** UP	2.25 (1.36 to 3.71)	0.00074	2	GSE22432 CDC versus common DC progenitor DN	1.21 (0.57 to 2.59)	0.52
Mitochondrial membrane	4.27 (1.71 to 10.6)	0.00091	11	GO regulation of mitochondrial membrane potential	1.97 (0.74 to 5.22)	0.63
GO **collagen trimer**	3.28 (1.52 to 7.07)	0.0012	3	GO collagen trimeR	1.86 (1.02 to 3.38)	0.062

Rows are ordered by the discovery p value.
*Bold fonts indicate the key phrase for name matching.
†P values are uncorrected for multiple testing.
‡The near-match confirmation p value (Pnmc) has been corrected for testing multiple matches for each candidate set, but not corrected for testing ten candidate sets. ** indicate significance after correction for testing 10 candidate sets.
CDC, conventional dendritic cell; DC, dendritic cell; DN, down; *FOXP3*, forkhead box p3; GO, Gene Ontology; IL2, interleukin-2; KO, knockout; OR, odds ratio obtained from Firth's penalized logistic regression; UP, up; WT, wild type.

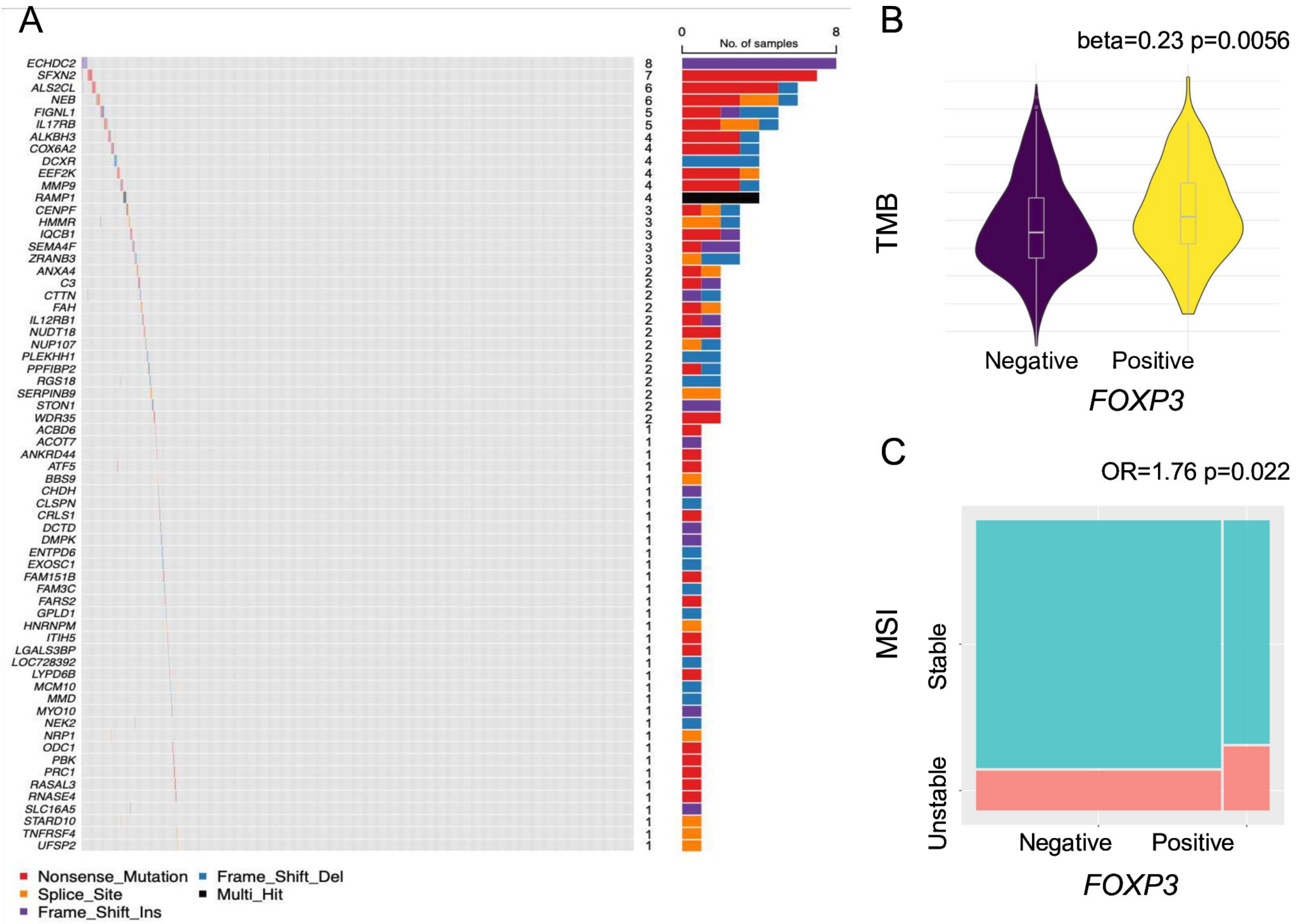

Figure 2 Oncology Research Information Exchange Network urinary tract cancer patients carrying germline truncating variants in forkhead box p3 (*FOXP3*)-related genes. (A) Oncoplot of germline variants in the 65 *FOXP3*-related genes. (B) Difference in tumor mutation burden (TMB). Beta and p value were obtained from a quantile regression adjusting for age and sex. (C) Difference in microsatellite instability (MSI). OR and p value were obtained from a logistic regression adjusting for age and sex.

enriched term associated with the 65 *FOXP3*-related genes (corrected p=0.013) (online supplemental table S6).

To substantiate this finding molecularly, we compared the transcriptomes between carriers and non-carriers of *FOXP3*-related variants. Among the 140 samples subjected to transcriptome analysis, 13 harbored a germline truncating variant in one of the 65 *FOXP3*-related genes. Interestingly, these patients had a significantly lower expression of the *FOXP3* RNA (figure 3A). This observation supports using *FOXP3* expression level as an indicator for studying the function of the *FOXP3*-related gene set. We divided the 140 ORIEN patients into two groups based on *FOXP3* expression levels, separated by the median value. The two groups were balanced concerning potential confounders: age of specimen collection, sex, race, upper versus lower urinary tract location, urothelial versus non-urothelial histology, and stage (online

Table 2 Epistasis between *FOXP3* and MMR pathways identified from germline exomes

Pathways*	Cases	Controls	OR (95% CI)	P value
None	478 (76.2%)	883 (83.1%)	Reference	Reference
MMR	66 (10.5%)	151 (14.2%)	0.84 (0.55 to 1.28)	0.42
FOXP3	56 (8.9%)	27 (2.5%)	3.68 (1.81 to 7.51)	<0.001
FOXP3 and MMR	10 (1.6%)	1 (0.094%)	25.2 (0.63 to 998)	0.086

Regression was adjusted for ancestry.
*Patients were separated into four groups by the level of germline variant carrier status. Level 1 did not carry any variants in the *FOXP3* nor the MMR pathway; level 2 carried deleterious variants in the MMR pathway, level 3 carried truncating variants in the *FOXP3*-related genes, and level 4 carried deleterious variants in the MMR and truncating variants in the *FOXP3*-related genes.
FOXP3, forkhead box p3; MMR, mismatch repair.

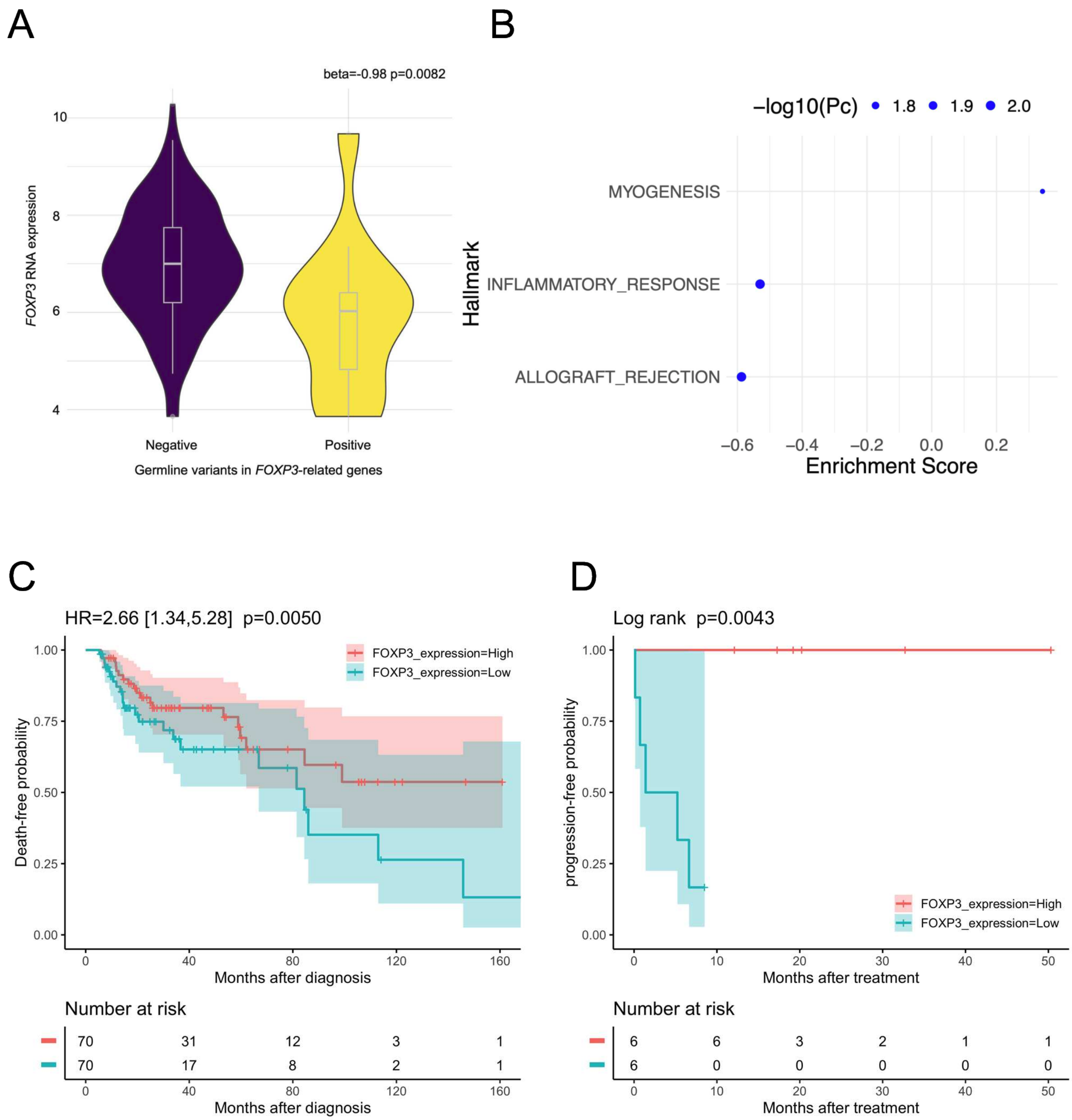

Figure 3 Transcriptional expression of *FOXP3* in urinary tract cancer. Results were derived from an analysis of 140 tumor RNA-seq samples in Oncology Research Information Exchange Network. (A) Patients carrying a germline variant in the 65 *FOXP3*-related genes had a lower expression of *FOXP3*. Beta and p value were obtained from a linear regression adjusting for age and sex. (B) Enriched pathways in carriers of germline variants in the 65 *FOXP3*-related genes. (C) Patients with lower *FOXP3* expression had a worse overall survival. (D) Patients with lower *FOXP3* expression had a worse progression-free survival following treatment with immune checkpoint inhibitors.

supplemental table S7). Additionally, we used the TCGA-BLCA dataset to cross-validate our findings.

Comparing the transcriptome profiles between the *FOXP3*-high and *FOXP3*-low tumors identified 757 differentially expressed genes (DEG) with an adjusted p value<0.05 (online supplemental figure S8). Among these, 563 were upregulated in the *FOXP3*-high patient group, and 194 were downregulated (online supplemental figure S8). GSEA showed that the DEGs were enriched with the "allograft rejection" pathway and immune pathways such as the "IL6 JAK STAT3 signaling" and "inflammatory response" (online supplemental figure S9A,C). The *FOXP3*-low tumors were immunologically cold (characterized by the lack of immune cell infiltration) compared with *FOXP3*-high tumors. These enrichments were replicated in the TCGA-BLCA. Even the strength of enrichment was similar (online supplemental figure S9B,D). Pathways negatively associated with *FOXP3* expression included "*MYC* targets v2" and "oxidative phosphorylation" (OXPHOS) (online supplemental figure S9A,B). Gene Set Variation Analysis[35] confirmed the correlation between high *FOXP3* expression and regulatory T-cell infiltration within the tumors (online supplemental figure S10).

To establish the association between germline variants in the 65 *FOXP3*-related genes and TME, we assessed each tumor's transcriptome, comparing those with *FOXP3*-related germline variants and those without, followed by a GSEA. Results showed that tumors harboring such variants displayed a negative correlation with "allograft rejection" and "inflammatory response" pathways (figure 3B). These findings suggest a link between germline variants and immunologically cold TME, highlighting the potential use of germline sequencing for predicting TME.

The expression of *FOXP3* is associated with clinical prognosis

The *FOXP3*-low group was associated with a worse OS, with a hazard ratio (HR) of 2.66 (p=0.0050) obtained from a Cox proportional hazards regression adjusted for age, sex, and stage (figure 3C). Dividing patients into treatment subgroups, those with low *FOXP3* expression exhibited poorer PFS. Among patients treated with platinum-based drugs, the HR for *FOXP3*-low was 1.27 (0.50–3.25) (online supplemental figure S11). On treatment with ICI, Cox proportional hazards regression was not applicable due to the absence of progression among *FOXP3*-high patients. However, the Kaplan-Meier curve showed a poorer outcome in *FOXP3*-low patients, and the log-rank test yielded a p value of 0.0043 (figure 3D).

FOXP3 expression contributes to intertumor heterogeneity

We conducted an unsupervised analysis of the tumor transcriptomes from ORIEN and TCGA-BLCA to unveil the intrinsic subtyping of UTC tumors and their correlation with *FOXP3*. Intriguingly, *FOXP3* exhibited a correlation with the third principal component in ORIEN and the first principal component in TCGA-BLCA (online supplemental figure S12A,B), with a correlation score of −0.45 (p<0.001) and −0.61 (p<0.001), respectively (online supplemental figure S12C,D). This suggests that *FOXP3* is one of the major contributors to UTC's intertumor heterogeneity.

Subsequently, we investigated how *FOXP3* aligns with known UTC subclasses as categorized by the consensus muscle-invasive bladder cancer classifier.[36] The results indicated that tumors with high *FOXP3* expression were more likely to be of the basal/squamous subtype and less likely to be of the luminal-papillary subclass (online supplemental figure S12E,F). In addition, stroma-rich was also significantly associated with high *FOXP3* expression in TCGA-BLCA (online supplemental file 1), consistent with the higher immune infiltration in this subclass.

DISCUSSION

In this large WES dataset from multiple US cancer centers, we identified germline truncating variants in a set of *FOXP3*-related genes implicated in UTC susceptibility in 16% of the patients. These variants were associated with reduced tumor *FOXP3* expression (figure 3A), suggesting a role in tumorigenesis. Notably, we observed a significant epistatic interaction between *FOXP3*-related and MMR gene variants, implicating a synergistic mechanism in cancer susceptibility and immune evasion.

Forkhead box P3 (*FOXP3*), a critical transcription factor for regulatory T cells (Tregs), also plays a context-dependent role in tumor biology. While its immunosuppressive function in Tregs can promote tumor immune escape, *FOXP3* also acts as a tumor suppressor in epithelial cancers by repressing oncogenes such as *HER2*, *SKP1*, and *MYC*.[37,38] Our findings support this tumor-suppressive role: tumors with low *FOXP3* expression exhibited enrichment of the *MYC* and OXPHOS pathways (online supplemental figure S7A,B), both of which are associated with immune evasion and treatment resistance. OXPHOS promotes M2 macrophage polarization,[39] while *MYC* modulates both innate and adaptive immune responses.[40]

Positioned on the X chromosome in humans and mice, the *FOXP3* gene is of paramount importance, as evidenced by the severe autoimmune phenotypes observed in mice with *FOXP3* mutation, known as scurfy mice. Male scurfy mice typically face fatal multiorgan inflammation within weeks of birth. Our study revealed no deleterious or truncating germline variants in the *FOXP3* gene, consistent with its indispensable role in survival.

Importantly, *FOXP3*-related germline variants were associated with increased MSI (figure 2C), suggesting a functional interaction with MMR deficiency. This epistatic relationship may represent a novel mechanism of tumorigenesis, particularly relevant to Lynch syndrome. Structural studies have shown that *FOXP3* binds to microsatellite regions of the DNA via multimerization,[41] a process that is potentially disrupted by MSI. Thus, MMR deficiency may impair *FOXP3*'s chromatin regulatory functions, and low *FOXP3* expression in this context could exacerbate chromatin-level dysregulation.

The observed synergy effect between *FOXP3* and MMR pathways is a novel finding and holds potential significance in clinical genetic testing for UTC. Germline testing for *FOXP3* pathway variants may help stratify cancer susceptibility risk in patients with Lynch syndrome. The substantial increase in risk when germline variants in both pathways are present could justify a more vigilant surveillance approach. Moreover, MSI is a biomarker for response to ICI.[42] MMR-deficient tumors are associated with increased *FOXP3*+ Tregs, thought to be a response to increased immunogenicity and neoantigen load.[43,44] Conversely, the germline *FOXP3*-related variants appear to confer an immune evasive property to these tumors by generating a cold TME (figure 3B).

Low *FOXP3* expression in our study correlated with poor PFS on ICI (figure 3D) and luminal-papillary tumor subclass (online supplemental figure S10E,F). Similarly, the luminal-papillary class of UTC tumors was among the least likely to respond to ICI in the IMvigor 210 study (ClinicalTrials.gov ID NCT02108652).[36] These findings suggest the consideration of *FOXP3* functionality in selecting patients for ICI, especially those with MSI. Interestingly, *FOXP3* expression is regulated by chromatin remodeling complexes and may be epigenetically modulated for therapy, offering a future avenue for therapeutic modulation.[45]

While our study leverages a robust real-world dataset with integrated germline, tumor, and transcriptomic data, several limitations warrant consideration. Our sample size is limited for accurately estimating the OR of carrying germline variants in the *FOXP3* and MMR pathways (table 2). It is also insufficient for a stratified analysis to clarify the distinct contributions of germline versus somatic alterations to prognosis. The *FOXP3*-related gene set includes 65 genes, each with an individual p value<0.25. It is likely that some of these genes have reduced effect sizes or no true association, while other relevant genes may have been missed. Further validation in a larger, independent cohort is necessary to refine and more accurately define the list of truly associated genes. Additionally, because the ORIEN samples are mostly composed of European individuals, a larger cohort is required to establish the generalizability of these findings in other populations. Furthermore, evaluating *FOXP3*-related variants in other Lynch-associated cancers could further elucidate the broader relevance of this epistatic interaction.

The near-match confirmation approach helps mitigate the limited statistical power of GSRVAT to some extent. While key phrase matching can reliably identify biologically correlated gene sets, it is not scalable for large-scale analyses. Further methodological development is needed to enable its broader application in future studies.

Another limitation of our study is the use of *FOXP3* transcript expression as a proxy for *FOXP3* pathway activity, which may not fully reflect the downstream functional consequences of germline variation in *FOXP3*-related genes. This underscores the need to develop cell-type-specific, directionally coherent gene signatures to more accurately capture FOXP3 activity across relevant cell types in UTC. Furthermore, we did not perform expression quantitative trait loci analyses to assess whether the identified germline variants mechanistically regulate *FOXP3* expression, primarily due to their rarity and the limited statistical power of our cohort. While cell-type deconvolution of bulk RNA-seq offered insights into immune cell infiltration in UTC tumors, our study is limited in its ability to distinguish the expression of tumor *FOXP3* and Treg *FOXP3*, which would certainly be of importance in delineating the role of germline *FOXP3*-related gene variants in tumorigenesis. Future studies with single-cell and spatial transcriptomics to distinguish tumor-intrinsic *FOXP3* from Treg-derived expression would be informative.

We did not evaluate treatment-related toxicity in this study, which may confound the observed survival outcomes by obscuring whether poor responses reflect true resistance or intolerance to therapy. Incorporating detailed clinical data on adverse events, dose delays, and treatment discontinuation will be essential to disentangle these effects.

In conclusion, our analysis uncovers a novel mechanism of UTC susceptibility involving truncating germline variants in a set of *FOXP3*-related genes, and their epistatic relationship with the MMR pathway. These variants are associated with reduced *FOXP3* expression in tumors, which in turn correlates with immune-evasive and stem cell-like phenotypes. Integrating germline testing for *FOXP3*-related variants with tumor *FOXP3* expression profiling may offer a path toward more precise risk stratification and therapeutic targeting in UTC.

Author affiliations
[1]Dermatology, University of Utah Health, Salt Lake City, Utah, USA
[2]University of Utah Health Huntsman Cancer Institute, Salt Lake City, Utah, USA
[3]National TeleOncology Program, Clinical Cancer Genetics Service, Durham VA Medical Center, Durham, North Carolina, USA
[4]Pharmacy, University of Kentucky, Lexington, Kentucky, USA
[5]Rutgers Cancer Institute of New Jersey, New Brunswick, New Jersey, USA
[6]The Ohio State University Comprehensive Cancer Center, Columbus, Ohio, USA
[7]Department of Surgery, Roswell Park Comprehensive Cancer Center, Buffalo, New York, USA
[8]Lafayette Family Cancer Center, Brewer, Maine, USA
[9]Aster Insights, Hudson, Florida, USA
[10]University of Colorado Cancer Center, Aurora, Colorado, USA
[11]University of Southern California Norris Comprehensive Cancer Center, Los Angeles, California, USA
[12]Department of Translational Genomics, University of Southern California Keck School of Medicine, Los Angeles, California, USA
[13]University of Iowa Holden Comprehensive Cancer Center, Iowa City, Iowa, USA
[14]Indiana University Melvin and Bren Simon Comprehensive Cancer Center, Indianapolis, Indiana, USA
[15]Department of Genitourinary Oncology, Moffitt Cancer Center, Tampa, Florida, USA
[16]University of Virginia School of Medicine, Charlottesville, Virginia, USA
[17]Department of Urology, University of Iowa Roy J. and Lucille A. Carver College of Medicine, Iowa City, Iowa, USA
[18]Genitourinary Oncology, H. Lee Moffitt Cancer Center and Research Center Inc, Tampa, Florida, USA
[19]George E. Wahlen Department of Veterans Affairs Medical Center, Salt Lake City, Utah, USA

Acknowledgements We acknowledge the Utah Genetic Reference Project, the University of Utah's Center for Genomic Medicine, for providing healthy controls for this study. We are grateful to the patients, their family members, and all research staff who supported the conduct of the Total Cancer Care protocol and the ORIEN Avatar project.

Contributors Conception and design of the work: B-JF and SG. Acquisition and interpretation of data: B-JF, WK, DAN, AA, KMB, CC, CJS, JK, EAS, GR, SE, KKS, MC, LG, BS, ASa, YZ, BPS, RJ, LB, CAM, KN, ASh, JC, BRC, and SG. Analysis of data: B-JF, WK, DAN, AA, KMB, CC, CJS, MC, and SG. Drafting and critical review: All authors. Final approval: All authors. Accountability: All authors. Guarantor: SG.

Funding The research reported in this article was partly supported by the U.S. Department of Veterans Affairs Merit Review Award #1T01 BX005765 (to SG). The contents do not represent the views of the U.S. Department of Veterans Affairs or the United States Government. Research reported in this publication was supported in part by the Huntsman Cancer Foundation and made use of the Genetic Counseling, High-Throughput Genomics and Cancer Bioinformatics, and

Cancer Biostatistics Shared Resources at Huntsman Cancer Institute, University of Utah. It was supported by the National Cancer Institute of the National Institutes of Health under award number P30CA042014. The computational resources used were partially funded by the NIH Shared Instrumentation Grant 1S10OD021644-01A1. The authors gratefully acknowledge the Chan Soon Shiong Family Foundation for providing the funds for sequencing the Heritage 1000 Projects samples.

Competing interests The PERCH software, for which B-JF is the inventor, has been non-exclusively licensed to Ambry Genetics Corporation for their clinical genetic testing services and research. B-JF also reports funding and sponsorship to his institution on his behalf from Pfizer and Regeneron Genetics Center. JK reports grant support from Loxo@lilly and ArtemiLife, ownership of Helix Diagnostics and VesiCure Technologies. RJ receives honoraria from FLASCO, Curio Science, DAVA Oncology, NCCN/Pfizer, and OncLive/MJH Life Sciences; provides consulting for AVEO, Bristol Myers Squibb, Sanofi, EMD Serono, Gilead Sciences, IDEOlogy Pfizer, and Seattle Genetics/Astellas; receives research funding from Bristol Myers Squibb, Gilead Sciences, and NCI. GR serves on an Advisory Board for AstraZeneca. SG has received research funding to the institute from Mirati Therapeutics, Novartis, Pfizer, Viralytics, Hoosier Cancer Research Network, Rexahn Pharmaceuticals, Five Prime Therapeutics, Incyte, MedImmune, Merck, Bristol Myers Squibb, Clovis Oncology, LSK BioPharma, QED Therapeutics, Daiichi Sankyo/Lilly, Immunocore, Seattle Genetics, Astellas, Acrotech and AstraZeneca. JC has advisory work at Aveo, Exelixis, Pfizer, Eisai, and MyCaregorythm, and research funding to the institution from Pfizer. YZ is on the Advisory Board for Bristol Myers Squibb, Amgen, Roche Diagnostics, Novartis, Janssen, Eisai, Exelixis, Castle Bioscience, Genzyme Corporation, Astrazeneca, Array, Bayer, Pfizer, Clovis, EMD Serono, Myovant, Data Safety and Monitoring Committee for Janssen Research and Development, received grant or research or clinical trial support from NewLinkGenetics, Pfizer, Exelixis, Eisai, and received consultant honorarium from Pfizer and Novartis. MC is employed by Aster Insights. BRC is a founder of Paterna Biosciences. The remaining authors declare no potential conflicts of interest relevant to this article.

Patient consent for publication Not applicable.

Ethics approval This study involves human participants. All patients have consented to the same protocol, Total Cancer Care, approved by the institutional review board (IRB) of each ORIEN cancer center. University of Utah IRB #00094497 approved this study. The IRB exempted this study based on exemption category 7. This category is “storage of identifiable information or biospecimens for secondary research use. Broad consent and limited IRB review are required”. Participants gave informed consent to participate in the study before taking part.

Provenance and peer review Not commissioned; externally peer reviewed.

Data availability statement Data may be obtained from a third party and are not publicly available. The data used in this research were generated through private funding by Aster Insights (www.asterinsights.com) in collaboration with the Oncology Research Information Exchange Network (ORIEN, www.oriencancer.org). Requests for access to the data used in this study can be submitted to the corresponding author and ResearchDataRequest@AsterInsights.com.

ORCID iDs

Bing-Jian Feng http://orcid.org/0000-0002-6669-6640
Courtney Carroll http://orcid.org/0000-0003-4906-549X
Yousef Zakharia http://orcid.org/0000-0001-9480-2626
Lindsey Byrne http://orcid.org/0000-0001-7131-5331
Sumati Gupta http://orcid.org/0000-0001-6271-0831

REFERENCES

1 Chamie K, Litwin MS, Bassett JC, *et al*. Recurrence of high-risk bladder cancer: a population-based analysis. *Cancer* 2013;119:3219–27.
2 Powles T, Valderrama BP, Gupta S, *et al*. Enfortumab Vedotin and Pembrolizumab in Untreated Advanced Urothelial Cancer. *N Engl J Med* 2024;390:875–88.
3 van der Heijden MS, Sonpavde G, Powles T, *et al*. Nivolumab plus Gemcitabine-Cisplatin in Advanced Urothelial Carcinoma. *N Engl J Med* 2023;389:1778–89.
4 Rosenberg JE, Hoffman-Censits J, Powles T, *et al*. Atezolizumab in patients with locally advanced and metastatic urothelial carcinoma who have progressed following treatment with platinum-based chemotherapy: a single-arm, multicentre, phase 2 trial. *Lancet* 2016;387:1909–20.
5 Massard C, Gordon MS, Sharma S, *et al*. Safety and Efficacy of Durvalumab (MEDI4736), an Anti-Programmed Cell Death Ligand-1 Immune Checkpoint Inhibitor, in Patients With Advanced Urothelial Bladder Cancer. *J Clin Oncol* 2016;34:3119–25.
6 Powles T, Eder JP, Fine GD, *et al*. MPDL3280A (anti-PD-L1) treatment leads to clinical activity in metastatic bladder cancer. *Nature New Biol* 2014;515:558–62.
7 Plimack ER, Bellmunt J, Gupta S, *et al*. Safety and activity of pembrolizumab in patients with locally advanced or metastatic urothelial cancer (KEYNOTE-012): a non-randomised, open-label, phase 1b study. *Lancet Oncol* 2017;18:212–20.
8 Liow E, Tran B. Precision oncology in urothelial cancer. *ESMO Open* 2020;5:e000616.
9 Powles T, Carroll D, Chowdhury S, *et al*. An adaptive, biomarker-directed platform study of durvalumab in combination with targeted therapies in advanced urothelial cancer. *Nat Med* 2021;27:793–801.
10 Loriot Y, Necchi A, Park SH, *et al*. Erdafitinib in Locally Advanced or Metastatic Urothelial Carcinoma. *N Engl J Med* 2019;381:338–48.
11 Saginala K, Barsouk A, Aluru JS, *et al*. Epidemiology of Bladder Cancer. *Med Sci (Basel)* 2020;8:15.
12 Martin C, Leiser CL, O’Neil B, *et al*. Familial Cancer Clustering in Urothelial Cancer: A Population-Based Case-Control Study. *J Natl Cancer Inst* 2018;110:527–33.
13 Hanson HA, Leiser CL, O’Neil B, *et al*. Harnessing Population Pedigree Data and Machine Learning Methods to Identify Patterns of Familial Bladder Cancer Risk. *Cancer Epidemiol Biomarkers Prev* 2020;29:918–26.
14 Mucci LA, Hjelmborg JB, Harris JR, *et al*. Familial Risk and Heritability of Cancer Among Twins in Nordic Countries. *JAMA* 2016;315:68.
15 Skeldon SC, Semotiuk K, Aronson M, *et al*. Patients with Lynch syndrome mismatch repair gene mutations are at higher risk for not only upper tract urothelial cancer but also bladder cancer. *Eur Urol* 2013;63:379–85.
16 Nassar AH, Abou Alaiwi S, AlDubayan SH, *et al*. Prevalence of pathogenic germline cancer risk variants in high-risk urothelial carcinoma. *Genet Med* 2020;22:709–18.
17 Kiemeney LA, Sulem P, Besenbacher S, *et al*. A sequence variant at 4p16.3 confers susceptibility to urinary bladder cancer. *Nat Genet* 2010;42:415–9.
18 Kiemeney LA, Thorlacius S, Sulem P, *et al*. Sequence variant on 8q24 confers susceptibility to urinary bladder cancer. *Nat Genet* 2008;40:1307–12.
19 Rothman N, Garcia-Closas M, Chatterjee N, *et al*. A multi-stage genome-wide association study of bladder cancer identifies multiple susceptibility loci. *Nat Genet* 2010;42:978–84.
20 Rafnar T, Vermeulen SH, Sulem P, *et al*. European genome-wide association study identifies SLC14A1 as a new urinary bladder cancer susceptibility gene. *Hum Mol Genet* 2011;20:4268–81.
21 Vosoughi A, Zhang T, Shohdy KS, *et al*. Common germline-somatic variant interactions in advanced urothelial cancer. *Nat Commun* 2020;11:6195.
22 Little J, Higgins JPT, Ioannidis JPA, *et al*. STrengthening the REporting of Genetic Association Studies (STREGA)— An Extension of the STROBE Statement. *STrengthening the REporting of Genetic Association Studies* 2009;6. Available: https://stacks.cdc.gov/view/cdc/50845
23 Dalton WS, Sullivan D, Ecsedy J, *et al*. Patient Enrichment for Precision-Based Cancer Clinical Trials: Using Prospective Cohort Surveillance as an Approach to Improve Clinical Trials. *Clin Pharmacol Ther* 2018;104:23–6.
24 Rosario SR, Dong B, Zhang Y, *et al*. Metabolic Dysregulation Explains the Diverse Impacts of Obesity in Males and Females with Gastrointestinal Cancers. *IJMS* 2023;24:10847.
25 Aster insights. ORIEN; 2024. Available: https://www.oriencancer.org

26 Kohlmann W, Nix DA, Pauley K, *et al*. Inherited Germline Variants in Urinary Tract Cancer: A Multicenter Whole-Exome Sequencing Analysis and Correlation With Clinical Features and Tumor Genomics. *JCO Precis Oncol* 2024;8:e2300697.
27 Ostrander BEP, Butterfield RJ, Pedersen BS, *et al*. Whole-genome analysis for effective clinical diagnosis and gene discovery in early infantile epileptic encephalopathy. *NPJ Genom Med* 2018;3:22.
28 Dobin A, Davis CA, Schlesinger F, *et al*. STAR: ultrafast universal RNA-seq aligner. *Bioinformatics* 2013;29:15–21.
29 Liao Y, Smyth GK, Shi W. featureCounts: an efficient general purpose program for assigning sequence reads to genomic features. *Bioinformatics* 2014;30:923–30.
30 Hu Y, Chung V, Comjean A, *et al*. BioLitMine: Advanced Mining of Biomedical and Biological Literature About Human Genes and Genes from Major Model Organisms. *G3 Genes|Genomes|Genetics* 2020;10:4531–9.
31 Feng B-J, Carroll C, Tejasvi T, *et al*. Exome-guided proteomic analysis identifies early biomarkers for the progression from psoriasis to psoriatic arthritis. *SSRN* [Preprint] 2023.
32 Feng B-J. PERCH: A Unified Framework for Disease Gene Prioritization. *Hum Mutat* 2017;38:243–51.
33 Wang K, Li M, Bucan M. Pathway-based approaches for analysis of genomewide association studies. *Am J Hum Genet* 2007;81:1278–83.
34 Miller DT, Lee K, Chung WK, *et al*. ACMG SF v3.0 list for reporting of secondary findings in clinical exome and genome sequencing: a policy statement of the American College of Medical Genetics and Genomics (ACMG). *Genet Med* 2021;23:1381–90.
35 Hänzelmann S, Castelo R, Guinney J. GSVA: gene set variation analysis for microarray and RNA-seq data. *BMC Bioinformatics* 2013;14:7.
36 Kamoun A, de Reyniès A, Allory Y, *et al*. A Consensus Molecular Classification of Muscle-invasive Bladder Cancer. *Eur Urol* 2020;77:420–33.
37 Wang J, Gong R, Zhao C, *et al*. Human FOXP3 and tumour microenvironment. *Immunology* 2023;168:248–55.
38 Wang L, Liu R, Ribick M, *et al*. FOXP3 as an X-linked tumor suppressor. *Discov Med* 2010;10:322–8.
39 Jiang L, Yu H, Ness S, *et al*. Comprehensive Analysis of Co-Mutations Identifies Cooperating Mechanisms of Tumorigenesis. *Cancers (Basel)* 2022;14:415.
40 Li J, Dong T, Wu Z, *et al*. The effects of MYC on tumor immunity and immunotherapy. *Cell Death Discov* 2023;9:103.
41 Zhang W, Leng F, Wang X, *et al*. FOXP3 recognizes microsatellites and bridges DNA through multimerization. *Nature New Biol* 2023;624:433–41.
42 Eso Y, Shimizu T, Takeda H, *et al*. Microsatellite instability and immune checkpoint inhibitors: toward precision medicine against gastrointestinal and hepatobiliary cancers. *J Gastroenterol* 2020;55:15–26.
43 Asaka S, Yen T-T, Wang T-L, *et al*. T cell-inflamed phenotype and increased Foxp3 expression in infiltrating T-cells of mismatch-repair deficient endometrial cancers. *Mod Pathol* 2019;32:576–84.
44 Michel S, Benner A, Tariverdian M, *et al*. High density of FOXP3-positive T cells infiltrating colorectal cancers with microsatellite instability. *Br J Cancer* 2008;99:1867–73.
45 Loo C-S, Gatchalian J, Liang Y, *et al*. A Genome-wide CRISPR Screen Reveals a Role for the Non-canonical Nucleosome-Remodeling BAF Complex in Foxp3 Expression and Regulatory T Cell Function. *Immunity* 2020;53:143–57.